Photophysical Properties of TiO_2 Surfaces Modified with Dinuclear RuRu and RuOs Polypyridyl Complexes

Anthea C. Lees,[†,§] Cornelis J. Kleverlaan,[‡,||] Carlo. A. Bignozzi,[‡] and Johannes G. Vos*[,†]

National Centre for Sensor Research, School of Chemical Sciences, Dublin City University, Dublin 9, Ireland, and Dipartimento di Chimica, Università di Ferrara, Via L. Borsari 46, 44100 Ferrara, Italy

Received March 12, 2001

The photophysical properties of nanoporous TiO_2 surfaces modified with two new Ru(II)−(bpt)−Ru(II) and Ru(II)−(bpt)−Os(II) polypyridyl complexes are reported. These dyads have been prepared by a two-step synthetic pathway. In the first step, $[Ru(dcbpy)_2Cl_2]$, where dcbpy is 4,4′-dicarboxy-2,2-bipyridyl, was reacted with the bridging ligand 3,5-bis(pyridin-2-yl)-1,2,4-triazole (Hbpt) to yield the mononuclear precursor $Na_3[Ru(dcbpy)_2(bpt)]\cdot 3H_2O$. Subsequent reaction of this compound with either $[Ru(bpy)_2Cl_2]$ or $[Os(bpy)_2Cl_2]$ yields the Ru(II)−Ru(II) and Ru(II)−Os(II) dyads. Electrochemical data, together with time-resolved transient absorption spectroscopy and the investigation of the incident-photon-to-current-efficiency (IPCE), have been used to obtain a detailed picture of the photoinduced charge injection properties of these dyads. These measurements indicate that for the heterosupramolecular triad based on Ru(II)−(bpt)−Ru(II), the final product species obtained upon charge injection is TiO_2(e)−Ru(II)Ru(III). For the mixed metal Ru(II)−(bpt)−Os(II) dyad, both metal centers inject efficiently into the semiconductor surface and as a result TiO_2(e)−Ru(II)Os(III) is obtained as a single charge-separated product.

Introduction

It has been recognized for some time that for the successful design of molecular devices, the addressability and organization of the molecular components have to be considered. Many studies on photochemically driven supramolecular assemblies have been carried out in solution, but although the results obtained from these studies have been very exciting, addressability and organization issues cannot be solved in the solution phase. For this reason, there is an increasing interest in the investigation of photochemically active molecular assemblies bound to active solid semiconductor substrates.[1] This research has been motivated by the development of practical photovoltaic cells based on sensitized nanocrystalline TiO_2 surfaces by Grätzel and co-workers. Their studies have shown that by the combination of a solid substrate and a molecular component, practical devices can produced.[2]

These studies have shown that although the basic photophysical properties of the molecular components are maintained upon immobilization of a molecular component on a semiconducting surface, the interaction with the surface can greatly change the rate of the individual photophysical processes. For example, when bound to TiO_2, ruthenium polypyridyl complexes that are intrinsically photolabile in solution become photostable.[2] This change in behavior is explained by the very fast, subpicosecond charge injection from the excited state of the surface bound compound into the valence band of the semiconductor.[3] In addition to this fast injection, the back electron-transfer process is several orders of magnitude slower than the forward electron-transfer reaction, and as a result, effective charge separation is observed. This ability of the TiO_2 surface to assist in a long-lived charge separation has been one of the driving forces behind the work carried out in this area.

The photophysical processes of molecular dyads have been studied in great detail.[4] The observation in solution is that while efficient interaction between molecular components can be obtained, long-lived charge separation is much more difficult to obtain. These dyads studied normally incorporate a ruthenium-based photosensitizer covalently attached to metal centers, such as Os(II),[5] Re(I),[6] or Rh(III),[7] or to organic electron acceptors or donors, such as methyl viologen[8] and phenothiazine.[9] The structures of the mixed metal complexes investigated at TiO_2 are shown in Figure 1. Upon immobilization of a molecular dyad on the surface, a heterosupramolecular triad is obtained. In this assembly, the solid substrate is an active component,

* To whom correspondence should be addressed. E-mail: johannes.vos@dcu.ie. Fax: 353-1-7005503.

† Dublin City University.

‡ Università di Ferrara.

§ Present address: Department of Chemistry, Trinity College, Dublin 2, Ireland.

|| Present address: Institute for Molecular Chemistry, University of Amsterdam, The Netherlands.

(1) (a) Hagfeldt, A.; Grätzel, M. *Chem. Rev.* **1995**, *95*, 49. (b) Hagfeldt, A.; Grätzel, M. *Acc. Chem. Res*. **2000**, *33*, 296. (c) Bignozzi, C. A.; Argazzi, R.; Kleverlaan, C. J. *Chem. Soc. Rev*. **2000**, *29*, 87.

(2) (a) O'Regan, B.; Grätzel, M. *Nature* **1991**, *353*, 737. (b) Kohle, O.; Ruile, S.; Grätzel, M. *Inorg. Chem.* **1996**, *35*, 4779.

(3) (a) Hannappel, T.; Burfeindt, B.; Storck, W.; Willig, F. *J. Phys. Chem. B* **1997**, *101*, 6799. (b) Tachibana, Y.; Moser, J. E.; Grätzel, D. R.; Klug, D. R.; Durrant, J. R. *J. Phys. Chem. B* **1996**, *100*, 20056.

(4) Balzani, V.; Scandola, F. *Supramolecular Photochemistry*; Ellis Horwood: New York, 1991.

(5) Kleverlaan, C.; Alebbi, M.; Argazzi, R.; Bignozzi, C. A.; Hasselmann, G. M.; Meyer, G. J. *Inorg. Chem.* **2000**, *39*, 1342.

(6) Argazzi, R.; Bignozzi, C. A.; Heimer, T. A.; Meyer, G. J. *Inorg. Chem*. **1997**, *36*, 2.

(7) Kleverlaan, C. J.; Indelli, M. T.; Bignozzi, C. A.; Pavanin, L.; Scandola, F.; Hasselman, G. M.; Meyer, G. J. *J. Am. Chem. Soc*. **2000**, *122*, 2840.

(8) Will, G.; Boschloo, G.; Rao, S. N.; Fitzmaurice, D. *J. Phys. Chem*. **1999**, *103*, 8067.

(9) Argazzi, R.; Bignozzi, C. A.; Heimer, T. A.; Castellano, F. N.; Meyer, G. J. *J. Phys. Chem. B* **1997**, *101*, 2591.

10.1021/ic0102743 CCC: $20.00
Published on Web 09/05/2001

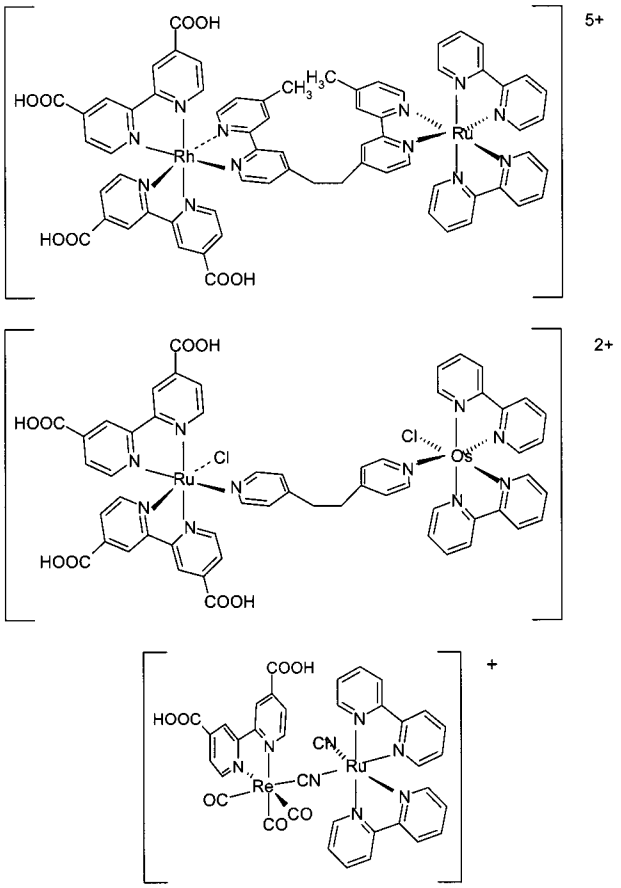

Figure 1. Structures of heteronuclear dyads from refs 5−7 that have been adsorbed on TiO_2.

and it is to be expected that the photophysical properties of the heterotriad will be different from those of the molecular dyad in solution. The studies of heterosupramolecular triads are aimed at improving our understanding of how the parameters that control electron injection into a semiconductor surface may be manipulated by variations in the composition of the attached molecular components. Another aspect of this work is to investigate how the electron- and energy-transfer pathways in molecular assemblies are modified upon attachment to a solid substrate and to assess the likelihood of long-lived charge separation over a substantial distance.

In this contribution, the photophysical properties of two dinuclear ruthenium- and osmium-containing polypyridyl complexes immobilized on nanocrystalline TiO_2 surfaces will be reported. The compounds are based on the bridging ligand 3,5-bis-(pyridin-2-yl)-1,2,4-triazole (Hbpt) (see Figure 2). Both homonuclear and heteronuclear ruthenium and osmium complexes of this ligand have been studied in solution. Electrochemical studies have shown that in the presence of the deprotonated bpt^- bridge, the interaction between the two metal centers is strong. Photophysical measurements have shown that for the mixed metal ruthenium−osmium compound, efficient energy transfer takes place from the ruthenium center to the osmium moiety. An important difference between the bpt-based compounds and those shown in Figure 1 is that the bpt bridge is very rigid and will not allow rotation around the linker.

Experimental Part

Materials. $[RuCl_3 \cdot H_2O]$ (Oxkem Ltd) and 4,4′-dimethyl-2,2′-bipyridine (Aldrich) were used without further purification. The solvents for the spectroscopic measurements, acetonitrile (MeCN) (Aldrich) and

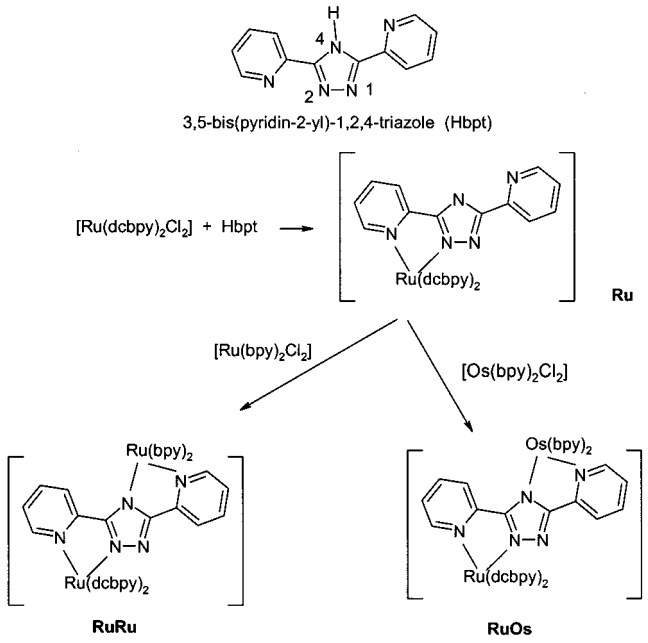

Figure 2. Structure of the bridging ligand Hbpt and synthetic routes.

methanol (MeOH) (Aldrich), were of spectroscopy grade and were used as received. 4,4′-Dicarboxy-2,2′-bipyridine (dcb) was prepared by the method of Oki *et al.*[10] The ligand Hbpt was available from earlier studies. The complexes *cis*-$[Ru(dcb)_2(Cl_2)]$,[11] *cis*-$[Os(bpy)_2Cl_2]\cdot 2H_2O$,[12] and *cis*-$[Ru(bpy)_2Cl_2]\cdot 2H_2O$[13] were prepared according to literature procedures.

Synthesis of $Na_3[Ru(dcb)_2(bpt)]\cdot 3H_2O$ (Ru). Hbpt (7.6×10^{-4} M) was heated under reflux in a basic solution of 2:1 ethanol/water (ca. 20 mL) to which the $[Ru(dcb)_2(Cl_2)]$ (7.5×10^{-4} M) was added. The mixture was further heated under reflux for 4−5 h, and the reaction was monitored by HPLC. The volume of the solution was reduced (ca. 10 mL) by rotary evaporation, and the product was precipitated by lowering the pH to 2.7 with HCl (ca. 2 mL, 0.2 M). Purification was achieved by dissolving the product obtained in water at pH 7 and utilizing column chromatography with Sephadex LH20 resin. Isolation of the product after chromatography was achieved by adjusting the pH with HCl as before. UV/vis aqueous pH = 8; $\lambda_{max} = 486$ nm; $\log \epsilon = 3.84$. ^{1}H NMR ([D$_6$]DMSO/NaOD 293 K): δ 8.82−8.75 (m, 4H, dcb-H_6), 8.44 (d, 1H, $H_{6''}$), 8.25 (d, 1H, $H_{3'}$), 7.95 (t, 1H, $H_{4'}$), 7.7−7.82 (m, 8H, dcb-H_3 and dcb-H_5), 7.65 (t, 1H, $H_{4''}$), 7.45 (d, 1H, $H_{3''}$), 7.28 (t, 1H, $H_{5'}$), 7.21 (t, 1H, $H_{5''}$). Yield = 75%. Elemental analysis for $Na_3[Ru(dcbpy)_2(bpt)]\cdot 3H_2O$ (**Ru**) calcd: C, 46.80; H, 3.46; N, 13.65. Found: C, 46.77; H, 3.11; N, 13.29. MS: 814.27 (calcd 813.72) for $H[Ru(H_2dcbpy)_2(Hbpt)]^+$.

Synthesis of $Na_4[Ru(dcb)_2(bpt)Ru(bpy)_2](PF_6)_3\cdot 5H_2O$ (RuRu). $Na_3[Ru(dcb)_2(bpt)]\cdot 3H_2O$ (4×10^{-4} M) was heated under reflux in a basic solution of 2:1 ethanol/water (ca. 40 mL) until dissolution occurred. To this was added $[Ru(bpy)_2(Cl_2)]\cdot 2H_2O$ (4×10^{-4} M) in a solution of 2:1 ethanol/water (ca. 20 mL). The resulting mixture was further heated under reflux for 8 h, and the reaction was monitored by HPLC. The volume of the solution was reduced to ca. 10 mL by rotary evaporation, and the product was precipitated by lowering the pH to 2.7 with HCl (ca. 2 mL, 0.2 M). Purification was achieved by dissolution of the complex in methanol/water containing NaOH (pH ca. 10) and utilization of column chromatography with Sephadex LH20 resin. Isolation of the product after chromatography was achieved by adjusting the pH with HCl as before and isolating the complex as the

(10) Oki, A. R.; Morgan, R. J. *Synth. Commun.* **1995**, *25*, 4093.
(11) Liska, P.; Vlachopoulos, N.; Nazeeruddin, M. K.; Comte, P.; Grätzel, M. *J. Am. Chem. Soc.* **1988**, *101*, 2591.
(12) Buckingham, D. A.; Dwyer, F. P.; Goodwin, H. A.; Sargeson, A. M. *Aust. J. Chem.* **1964**, *17*, 325.
(13) Sullivan, B. P.; Salmon, D. J.; Meyer, T. J. *Inorg. Chem.* **1978**, *17*, 3334.

PF_6 salt. Yield = 48%. Elemental analysis for $Na_4[Ru(dcbpy)_2(bpt)Ru(bpy)_2](PF_6)_3 \cdot 5H_2O$ (**RuRu**) calcd: C, 36.53; H, 2.49: N, 9.89. Found: C, 36.52; H, 2.41; N, 9.47. MS: 408.37 (calcd 408.38) for $[(H_2dcbpy)_2Ru(bpt)Ru(bpy)_2]^{3+}$; 612.14 (calcd 612.58) for $[(H_2dcbpy)_2Ru(bpt)Ru(bpy)_2]^{2+}$; 685.22 (calcd 685.07) for $\{[(Hxdcbpy)_2Ru(bpt)Ru(bpy)_2]PF_6\}^{2+}$. UV/vis aqueous pH = 8; λ_{max} = 456 nm; log ϵ = 4.24.

Synthesis of $Na_3[Ru(dcb)_2(bpt)Os(bpy)_2](PF_6)_2 \cdot 3H_2O$ (RuOs). $Na_4[Ru(dcb)_2(bpt)] \cdot 3H_2O$ (4×10^{-4} M) was heated under reflux in a basic solution of 2:1 ethanol/water (ca. 40 mL) until dissolution occurred. To this was added $[Os(bpy)_2(Cl_2)] \cdot 2H_2O$ (4×10^{-4} M) in a solution of 2:1 ethanol/water (ca. 20 mL) together with a small amount of zinc metal. The resulting mixture was further heated under reflux for 20 h, and the reaction was monitored by HPLC. The zinc metal was removed by gravity filtration, and the volume of solution was reduced to ca. 10 mL by rotary evaporation. The product was precipitated by lowering the pH to 2.7 with HCl (ca. 2 mL, 0.2 M) and subsequently isolated as the PF_6 salt. Purification was achieved by dissolution of the complex in methanol/water containing NaOH (ca. pH 10) and utilization of column chromatography with Sephadex LH20 resin. Isolation of the product after chromatography was achieved by adjusting the pH with HCl as before and isolating the complex as the PF_6 salt. Elemental analysis for $Na_3[Ru(dcbpy)_2(bpt)Os(bpy)_2](PF_6)_2 \cdot 3H_2O$ (**RuOs**) calcd: C, 39.18; H, 2.68; N, 10.61. Found: C, 39.27; H, 2.99; N, 10.04. MS: 329.80 (calcd 328.57) for $[(H_2dcbpy)_2Ru(bpt)Os(bpy)_2]^{4+}$; 437.98 (calcd 438.09) for $[(H_2dcbpy)_2Ru(bpt)Os(bpy)_2]^{3+}$; 656.70 (calcd 657.14) for $[(H_2dcbpy)_2Ru(bpt)Os(bpy)_2]^{2+}$; 729.78 (calcd 729.64) for $\{[(H_2dcbpy)_2Ru(bpt)Os(bpy)_2]PF_6\}^{2+}$. UV/vis aqueous pH = 8; λ_{max} = 471 nm; log ϵ = 4.31.

Coating Procedures. Coating of the TiO_2 surface with the dye was carried out by soaking the film for 3 h (transient absorption experiments) and 24 h (incident-photon-to-current-efficiency (IPCE) measurements) in a ca. 1×10^{-4} M methanol solution of each of the complexes. After completion of the dye adsorption, the film was rinsed with an excess of acetone and dried. The modified surfaces obtained in this manner will be referred to as **TiO_2−Ru**, **TiO_2−RuRu**, and **TiO_2−RuOs**, depending on the nature of the dyad. The measurements were performed directly after the preparation of the film.

Instrumentation. UV/vis spectra were recorded with a Kontron Uvikon 860 spectrophotometer. Emission spectra were measured on a SPEX Fluoromax 2 spectrofluorimeter equipped with a Hamamatsu R3896 tube. The emission spectra were corrected for the instrumental response. The NMR spectra were recorded on a Bruker AMX 400. HPLC was carried out on a Waters system equipped with a 990 photodiode array detector with a SAX anionic exchange column (8 mm × 100 mm) and 50:50 (MeCN/H_2O) 0.05 M phosphate buffer as the mobile phase. The TiO_2 films were prepared as described by Nazeeruddin et al.[14]

For the IPCE measurement, the TiO_2 was deposited on conductive fluorine-doped SnO_2 glass (LOF, ∼10 Ω/□), while for the transient absorption measurement normal glass was used. Cyclic voltammetry was carried out with an Autolab PG30 potentiostat using a three-electrode configuration. The reference used was SCE, and Pt was used as the counter electrode. The working electrode was a TiO_2 electrode coated as described above. All measurements were carried out in degassed (Ar) acetonitrile containing 0.3 M $LiClO_4$.

Photoelectrochemical measurements were performed in a two-electrode sandwich cell arrangement by using SnO_2/TiO_2/dye as photoanode (active area 0.5 cm^2) and a SnO_2/Pt-coated glass as counter electrode. The sandwich cell was filled with an acetonitrile solution containing 0.3 M LiI and 0.03 M I_2. The current measurements were performed with a Kontron DDM4021 digital multimeter. The excitation source was a 150 W Xe lamp coupled to a 0.22 m monochromator. Incident light flux was measured with a UDT-calibrated Si diode. Nanosecond flash photolysis transient absorption spectra were measured by irradiating the sample with 6−8 ns (fwhm) of a Continuum Surelight Nd:YAG laser (10 Hz repetition rate) and using as probe light a pulsed Xe lamp perpendicular to the laser beam. The excitation wavelength was obtained by frequency doubling (532 nm). The 150 W Xe lamp was equipped with an Applied Photophysics model 408 power supply and Applied Photophysics model 410 pulsing unit (giving pulses of 0.5 ms). A shutter, Oriel model 71445, placed between the lamp and the sample was opened for 100 ms to prevent PMT fatigue. Suitable pre- and postcutoff and band-pass filters were used to minimize the probe light and scatter light of the laser. The orientation of the films was 45° with respect to the laser and probe light and was set up in such a way that the scatter light was reflected to the probe light. In this way, we were also able to measure in the early time domain ($t <$ 50 ns) without measuring artifacts due to scatter light. The sampling rate was kept at a relatively long time (intervals of 10 s) to prevent electron accumulation in the conduction band of the semiconductor. The light was collected in a LDC Analytical monochromator, detected by a R928 PMT (Hamamatsu), and recorded on a LeCroy 9360 (600 MHz) oscilloscope. The laser oscillator, Q-switch, lamp, shutter, and trigger were externally controlled with a digital logic circuit, which allowed for synchronous timing.

The absorption transients were plotted as $\Delta A = \log(I_o/I_t)$ vs time, where I_o was the monitoring light intensity prior the laser pulse and I_t was the observed signal at delay time t. The same setup as described above was employed for the time-resolved emission experiments, with the exception that the probe lamp was not used.

Electrospray mass spectra were recorded using a VG Biotech Quattro instrument. The samples were dissolved in MeCN/water mixtures and injected with a flow rate of 10−20 μL/min. The cone voltage was 20 V.

Results

Both dinuclear compounds were prepared in a two-step process as shown in Figure 2. Earlier work has shown that in the mononuclear precursor obtained in the first reaction, the Hbpt ligand is coordinated to the N2 position of the central triazole ring of the bridge (Figure 2). A small amount of N4-coordinated material together with some dinuclear material is removed by chromatographic techniques.[15] So, because for both compounds the ruthenium carboxy grouping was coordinated first, both complexes are bound to the titanium oxide surface by a carboxy-containing metal center coordinated to a pyridine ring and the N2 nitrogen of the 1,2,4-triazole ring. Consequently, the $Ru(bpy)_2$ and $Os(bpy)_2$ moieties are bound to pyridine and the N4 atom of the triazole ring. Because of the presence of various acidic protons, the exact composition of the compounds in the solid state is often difficult to determine. They are obtained as sodium salts, but the amount of sodium incorporated is not always the same and may depend on the manner in which the materials are precipitated. In our hands, the best results were obtained by precipitating the dinuclear metal complexes as PF_6 salts. Elemental analysis suggests that the mononuclear precursor is isolated as a neutral molecule in which three of the carboxy protons are replaced by sodium. The molecular composition of the compounds is furthermore confirmed by mass spectral data. The uncertainty in the composition of the compounds in the solid state does not however affect the measurements because in all cases the protonation state of the compounds in solution is controlled by the pH of the solutions.

The compounds obtained have been characterized both in solution and when immobilized on TiO_2. The UV/vis spectra in the visible region of **RuRu** and **RuOs** in aqueous solution at pH 7 are shown in Figure 3. Both compounds show ruthenium-based metal-to-ligand charge-transfer (MLCT) transitions in the 450 nm region, while for the osmium-containing compound, an additional absorption feature is observed at 650 nm. This

(14) Nazeeruddin, M. K.; Kay, M.; Rodicio, I.; Humphry-Baker, R.; Müller, E.; Liska, P.; Vlachopoulos, N.; Grätzel, M. *J. Am. Chem. Soc.* **1993**, *115*, 6382.

(15) Buchanan, B. E.; Wang, R.; Vos, J. G.; Hage, R.; Haasnoot, J. G.; Reedijk, J. *Inorg. Chem.* **1990**, *29*, 3263.

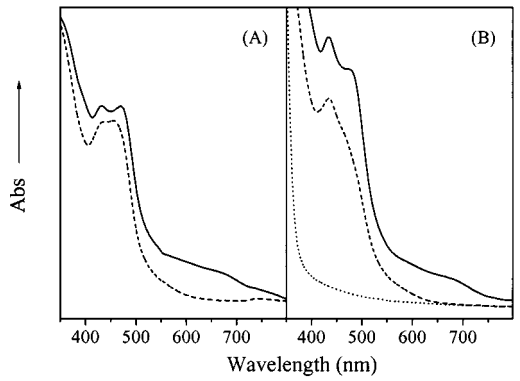

Figure 3. UV−vis absorption spectra of (A) **RuRu** (−) and **RuOs** (- - -) in aqueous solution at pH 7 (room temperature) and (B) **TiO_2−RuRu** (−), **TiO_2−RuOs** (- - -), and TiO_2 (···) in MeCN (room temperature).

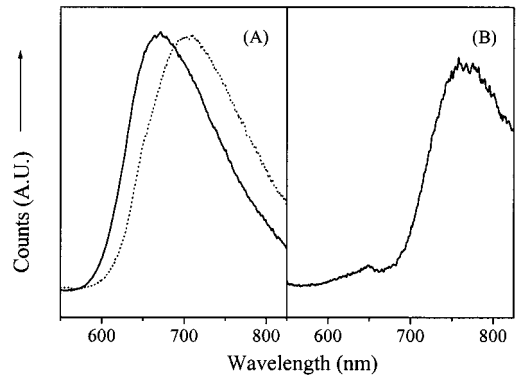

Figure 4. Emission spectra of (A) **RuRu** in aqueous solution at pH = 7 (−) (λ_{max} = 670 nm) and pH = 3 (- - -) (λ_{max} = 705 nm) and (B) **RuOs** (λ_{max} = 770 nm) in aqueous solution at pH 7 (room temperature).

latter absorption can be assigned to a transition from the osmium center to the ^{3}MLCT state. The mononuclear precursor shows an absorption maximum at 495 nm. The emission spectra of the dinuclear compounds at pH 3 and 7 are shown in Figure 4. At pH 7, **RuRu** shows an emission maximum at about 670 nm, while at pH 3, a value of 705 nm is observed. For **RuOs** at pH 7, a single emission signal is observed with a λ_{max} of 770 nm. These values are similar to those observed for the non-carboxy analogues of these compounds, for which values of 650 and 760 nm are obtained for the homonuclear ruthenium and ruthenium−osmium compounds, respectively.[16] For **Ru** in aqueous solution at pH 7, an emission maximum is observed at 690 nm. No major shift in the absorption features of the compounds is observed upon binding of the dyads to the TiO_2 surface. The heterosupramolecular triads do not however show any emission.

The electrochemical properties of the immobilized compounds are shown in Figure 5. The figure shows two well-defined metal-based oxidations at 1080 (ΔE = 75 mV) mV vs SCE and 1380 (ΔE = 110 mV) mV vs SCE for **RuRu**, while for **RuOs**, values of 660 (ΔE = 60 mV) mV and 1370 (ΔE = 110 mV) mV were obtained. Again, these values are in agreement with those reported for the non-carboxy complexes, and they indicate that there is substantial interaction between the two metal centers.[16] The data also suggest that there are no major changes in the electrochemistry going from the solution phase to the TiO_2 surface.

(16) Hage, R.; Haasnoot, J. G.; Nieuwenhuis, H. A.; Reedijk, J.; de Ridder, D. J. A.; Vos, J. G. *J. Am. Chem. Soc.* **1990**, *112*, 9245.

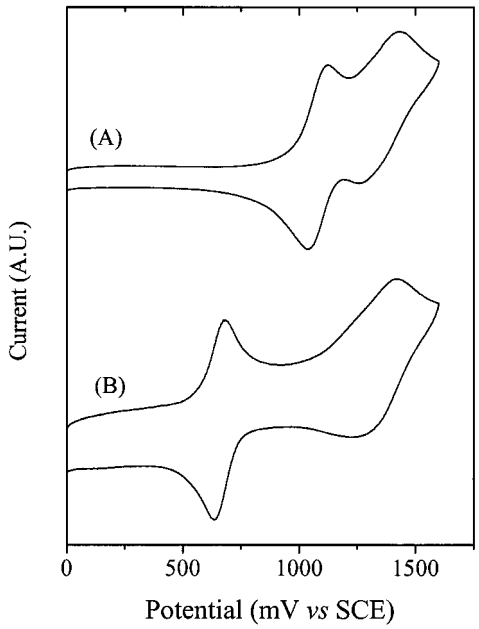

Figure 5. Cyclic voltammograms of (A) **TiO_2−RuRu** and (B) **TiO_2−RuOs**, with a surface coverage of $\Gamma \approx 1.0 \times 10^{14}$ molecules cm^{-2}, measured in MeCN 0.3 M in $LiClO_4$ vs SCE at a scan rate of ν = 50 mV s^{-1}.

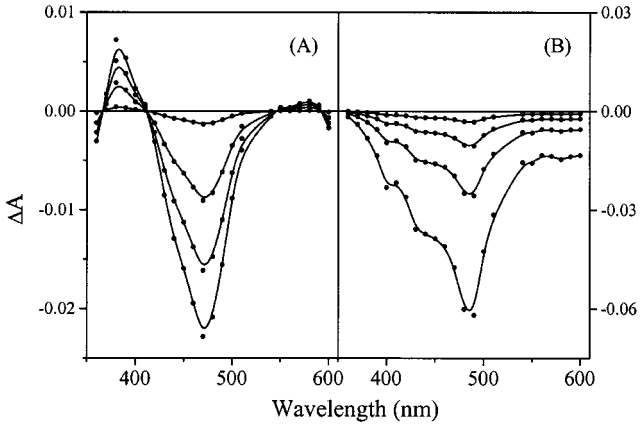

Figure 6. Time-resolved transient absorption spectra in aqueous solution (pH 7, room temperature) of (A) **RuRu** at τ_d = 10, 100, 250, and 750 ns (τ = 260 ns), top to bottom, and (B) **RuOs** at τ_d = 0, 15, 30, and 50 ns (τ = 20 ns), top to bottom, (λ_{exc} = 532 nm, P = 6.5 mJ/pulse).

The excited-state properties of **RuRu** and **RuOs** were investigated both in solution and on TiO_2. The transient absorption spectra in aqueous solution at pH 7 are shown in Figure 6, while the equivalent measurements on TiO_2 in CH_3CN are shown in Figure 7. Figure 6 shows for both compounds a bleaching in the 400−500 nm region and for **RuRu** the formation of a new transient species at about 350 nm. For **RuOs**, bleaching is also observed at 600 nm. In contrast, the TiO_2 data in Figure 7 do not indicate the formation of an absorption band at 350 nm. However, for both compounds, a bleaching is observed in the 400−500 nm region and in addition at 600 nm for the **RuOs** species. The IPCE of the compounds, as defined in eq 1, is shown in Figure 8.

$$\mathrm{IPCE}(\lambda) = \frac{1.24 \times 10^3\ (\mathrm{eV\ nm}) \times \mathrm{photocurrentdensity}\ (\mu\mathrm{A\ cm^{-2}})}{\mathrm{wavelength\ (nm)} \times \mathrm{photonflux}\ (\mu\mathrm{W\ cm^{-2}})} \quad (1)$$

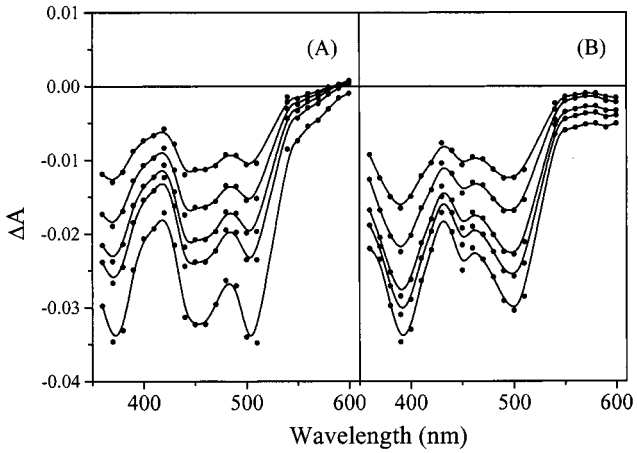

Figure 7. Time-resolved transient absorption spectra of the TiO_2 films in MeCN/0.1 M $LiOCl_4$ (room temperature), covered with (A) **TiO_2−RuRu** and (B) **TiO_2−RuOs** at τ_d = 10, 250, 500, 2000, and 5000 ns, top to bottom (λ_{exc} = 532 nm, P = 0.5 mJ cm^{-2}).

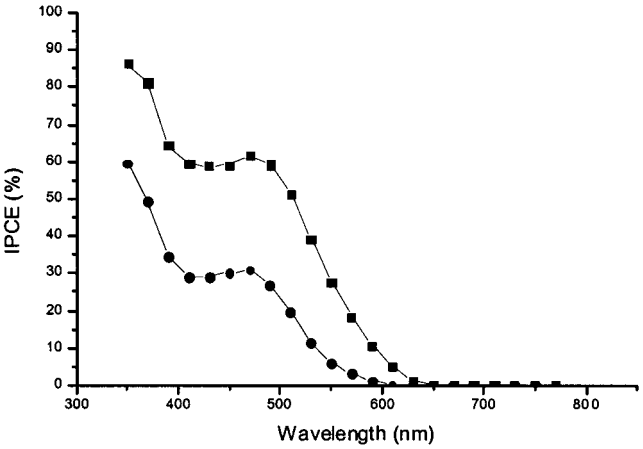

Figure 8. Incident-photon-to-current efficiency vs. the excitation wavelength, IPCE(λ), for (■) **TiO_2-Ru** and (●) **TiO_2-RuRu** measured in 0.3 M LiI and 0.03 M I_2. The optical density of the photoanodes at the adsorption maxima in the visible region was 0.9 for **TiO_2-Ru** and 1.1 for **TiO_2-RuRu**.

The spectra show that the IPCE is closely related to the absorption spectra of the compounds. The highest value of IPCE(λ) for both ruthenium complexes is obtained at their absorption maximum of 470 nm. Interestingly, for the dinuclear **RuRu** species, the IPCE obtained at this wavelength is 30%, about half of that observed for the mononuclear ruthenium compound (63%). For **RuOs** species, no appreciable photocurrent is obtained. To understand the processes determining the efficiency of the cell, experiments in the presence and absence of a electron scavenger were employed. The quenching of oxidized dye molecules by 0.3 M I^-, yielding in the parent complex an iodine radical and a TiO_2 nanoparticle with an electron excess, is shown in Figure 9 (trace 2 in parts A and B). The concentration of I^- was the same as that in typical cell conditions, while the concentration of Li^+ ions was kept constant (0.3 M $LiClO_4$) with respect to the recombination experiments (trace 1 in parts A and B). The scavenging of the oxidized form of **RuRu** is completed after ca. 20 ns, whereas the quenching of the oxidized form of **RuOs** is much slower (compare trace 2 in Figure 9A and trace 2 in Figure 9B).

Discussion

Spectroscopy in Solution. To determine the energetics of the molecular dyads, the group and excited-state properties of the dinuclear species were measured in solution. The absorption features of the two dinuclear compounds in solution and when immobilized on TiO_2 are very similar. This indicates that no substantial differences in the excited-state levels are expected upon immobilization. However, while both compounds emit strongly in solution, no emission is observed on TiO_2. The emission maxima observed for **RuRu** are pH-dependent, varying from 670 to 705 nm when changing the pH from 7 to 3, a change that is in agreement with protonation of the carboxy groupings. This indicates that for the **RuRu** dyad, the emitting state is based on the Ru(dcbpy)$_2$ moiety. This is as expected from the relative energies of the ^{3}MLCT levels of the bpy and dcbpy centers. So, upon excitation of the Ru(bpy)$_2$ center, energy transfer to the Ru(dcbpy)$_2$ moiety is observed, leading to a single emission for the molecular dyad in solution.

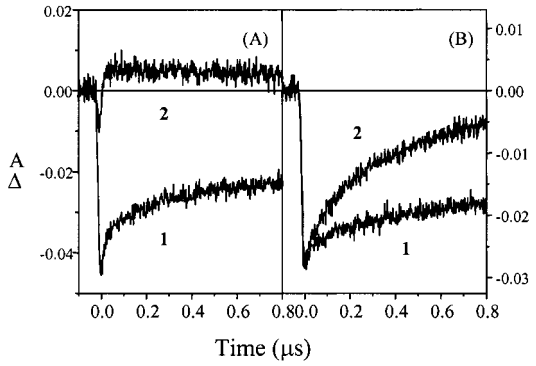

Figure 9. The microsecond decay kinetics measured at 480 nm of (A) **TiO_2−RuRu** and (B) **TiO_2−RuOs** measured in the presence of (1) MeCN/0.3 M $LiOCl_4$ and (2) MeCN/0.3 M LiI (λ_{exc} = 532 nm, P = 0.3 mJ cm^{-2}).

For **RuOs**, a single emission is observed at about 750 nm which is clearly Os-based. This is confirmed by the fact that this emission is not pH-dependent. So, upon excitation of the Ru(dcbpy)$_2$ moiety, efficient energy transfer to the osmium center is observed. This is confirmed by the transient absorption spectrum shown in Figure 6A. This spectrum shows the formation of an Os(III) center as indicated by the depletion at 600 nm. This is as expected and has been observed before for Ru−Os complexes.[5]

Redox Chemistry. For the **TiO_2−RuOs** triad, the assignment of the metal-based oxidations observed in Figure 5 is straightforward. Because Os polypyridyl complexes tend to have less positive M(II/III) redox processes than their ruthenium analogues, the oxidation at 0.66 V can be assigned to the Os center while the process at 1.37 V is assigned to the Ru(II/III) redox process. Interestingly, the peak-to-peak separation of the redox waves is 60 mV for the osmium-based redox couple but considerably larger at 110 mV for the ruthenium center. This difference is most likely explained by the complicated multistep acid−base chemistry of the carboxy ligands, which precludes the measurement of accurate redox potentials.

For **RuRu**, the assignment is less simple. Earlier experiments have shown that ruthenium polypyridyl centers bound to the N4 atom of bpt are more difficult to oxidize than the analogues coordinated to the N2 site by about 70 mV.[16,17] In addition, because of the increased π-acceptor properties of the carboxy ligands, it is expected that the Ru(dcbpy)$_2$ moiety is more difficult to oxidize than the Ru(bpy)$_2$ analogue. From earlier studies on ruthenium(dcbpy) complexes containing pyridyltriazole ligands, it was estimated that the redox potentials of the

(17) Hage, R.; Prins, R.; Haasnoot, J. G.; Reedijk, J.; Vos, J. G. *J. Chem. Soc., Dalton Trans.* **1986**, 253.

carboxy bpy analogues are between 100 and 150 mV higher than those observed for their non-carboxylated parent compounds.[18] This suggests that there will be a very small difference between the metal-based oxidation potentials of the two ruthenium sites in **RuRu**. On the basis of a comparison with literature data, it is therefore not possible to predict the location of the lowest oxidation potential. However, like for **RuOs**, one of the redox couples is much less reversible than the other and it is again the redox couple observed at 1.38 V vs SCE. This suggests that the latter redox process can be attributed to the carboxy center while the first redox process observed at 1.08 V is assigned to the non-carboxy center. The difference between the metal-based redox couples in **RuRu** is 300 mV. This value is identical to that observed for the non-carboxylated parent compound for which values of 1.04 and 1.34 V were obtained.[16] In the latter compound, the center with the lowest oxidation state is coordinated to the N2 site of the triazole ring. Because the difference in redox potentials between the two sites is the same, it is expected that the interaction between the two metal centers in the two compounds is very similar.

From these considerations, the following picture emerges. Upon excitation of the **RuOs** dyad, the emitting state is firmly based on the osmium site. Upon immobilization of this molecular dyad to TiO_2, this metal center will not be directly coupled to the oxide surface, so for the **RuOs** dyad, the energy-transfer pathway is away from the surface. Excitation of the **RuRu** dyad leads to an emission from a triplet state located at the carboxy ligands, a site that will be bound directly to the TiO_2 surface. So in this case, the energy-transfer pathway is toward the surface. In both dyads, the lowest metal-based oxidation is based on the unit bound to the N4 atom of the triazole ring, the unit that is not directly bound to the oxide surface upon immobilization. For the **RuOs** dyad, the difference between the redox potentials of the two centers is expected to be about 400 mV. For **RuRu**, a much smaller difference of less than 100 mV is however expected.

Electron Injection. A comparison of the absorption spectra obtained for the heterotriads with those of the solution-based dyads indicates that there are no major changes in the absorption features upon attachment to the semiconductor surface. However, a comparison of Figures 6 and 7 shows clearly that the excited-state behavior of the heterosupramolecular triad is substantially different from that of the molecular dyad in solution. There is no evidence for the formation of the dcbpy-based radical anion, which is characteristic for the excited-state absorption spectrum, as observed in solution. Instead, strong bleaches are observed at about 450 and 380 nm. These are assigned to bleaching of the Ru(II) MCLT bands. This assignment was confirmed by spectroelectrochemical measurements (not shown). This observation is in agreement with the absence of emission from both **RuRu** and **RuOs**. This indicates that for both triads, injection into the oxide surface is very efficient, resulting in reduced TiO_2 and an oxidized dye. The absence of an emission for **RuRu** is not all that surprising. It is generally assumed that upon excitation of a TiO_2-bound ruthenium complex, injection from the molecular component to the oxide surface occurs at the femtosecond time scale. Such a fast injection, resulting in the charge-separated state, is more favorable than population of the emitting triplet state. The absence of emission from **RuOs** is less straightforward. As already pointed out above, the energy-transfer pathway leads away from the TiO_2 surface to the osmium center. In the transient absorption experiments shown in Figures 6 and 7, the absorbances of **RuRu** and **RuOs** are the same at the excitation wavelength of 532 nm. At this wavelength, both the ruthenium and the osmium center will absorb. The surprising observation is that the amount of transient observed is the same in both experiments, because the amount of depletion observed is the same. In addition, a similar behavior for both triads is also observed in Figure 7. This strongly suggests that injection from the osmium moiety to the oxide surface is complete. This is indeed confirmed by the absence of any emission.

Considering that for the triads both metal centers are capable of absorption at 532 nm, two different reaction pathways need to be considered for each. The **TiO_2−RuRu** triad will be considered first. Excitation of this triad can lead to two different initial products as shown in reaction 2:

$$TiO_2-Ru(II)Ru(II) \rightarrow TiO_2-*Ru(II)Ru(II) + TiO_2-Ru(II)*Ru(II) \quad (2)$$

It is however expected that the second intermediate will within the nanosecond range be transformed into the first one. Injection from this state into the TiO_2 then takes place according to reaction 3:

$$TiO_2-*Ru(II)Ru(II) \rightarrow TiO_2(e)-Ru(III)Ru(II) \quad (3)$$

According to Figure 7, this injection is fast and within the laser pulse (<10 ns). According to the redox properties of the two moieties (see previous discussion), a final product species as shown in reaction 4 will be produced by electron transfer from the outer to the inner ruthenium center:

$$TiO_2(e)-Ru(III)Ru(II) \rightarrow TiO_2(e)-Ru(II)Ru(III) \quad (4)$$

A similar reaction sequence can be derived for **TiO_2−RuOs**. Excitation of this triad at 532 nm will yield two species as shown in reaction 5:

$$TiO_2-Ru(II)Os(II) \rightarrow TiO_2-*Ru(II)Os(II) + TiO_2-Ru(II)*Os(II) \quad (5)$$

At this stage, the behavior observed for the mixed metal triad becomes significantly different from that observed for the solution-based dyad. For the molecular dyad in solution, a well-defined osmium-based emission is observed; for the heterosupramolecular triad, no emission could be detected. The transient absorption data indicate that injection from the dyad into the oxide surface is fast (<10 ns) (reactions 6 and 7). An alternative

$$TiO_2-*Ru(II)Os(II) \rightarrow TiO_2(e)-Ru(III)Os(II) \quad (6)$$

$$TiO_2-Ru(II)*Os(II) \rightarrow TiO_2(e)-Ru(II)Os(III) \quad (7)$$

process for reaction 6 is energy transfer to the osmium moiety rather than into the semiconductor, as observed for **RuOs** in solution, resulting in $TiO_2-Ru(II)*Os(II)$. Furthermore, the formation of the charge-separated state $TiO_2-Ru(II)Os(III)$ in reaction 7 is not trivial. Because energy or electron transfer from **Os(II)* to the ruthenium center is energetically not favorable, the absence of any osmium-based emission indicates that remote injection into the semiconductor from the osmium center is likely to occur.[1c]

The redox chemistry shown in Figure 5 suggests that for both these products, the final species is expected to be $TiO_2(e)-Ru$-

(18) Lees, A. C.; Evrard, B.; Keyes, T. E.; Vos, J. G.; Kleverlaan, C. J.; Alebbi, M.; Bignozzi, C. A. *Eur. J. Inorg. Chem.* **1999**, *12*, 2309.

(II)Os(III). This can be formed from the Ru(III) intermediate produced in reaction 6 as shown in reaction 8:

$$TiO_2(e)-Ru(III)Os(II) \rightarrow TiO_2(e)-Ru(II)Os(III) \quad (8)$$

Charge Separation. One of the aims of studies involving solid components is to reduce the rate of back reaction. In nature, membranes are used to promote the forward and to slow the charge recombination. For the two triads, the charge recombination reactions are shown in reactions 9 and 10:

$$TiO_2(e)-Ru(II)Ru(III) \rightarrow TiO_2-Ru(II)Ru(II) \quad (9)$$

$$TiO_2(e)-Ru(II)Os(III) \rightarrow TiO_2-Ru(II)Os(II) \quad (10)$$

Figure 9 shows clearly that these processes are slow and take place on the microsecond time scale. Considering that the injection is faster than 10 ns, i.e., faster than the excited-state lifetime, a considerable degree of charge separation is obtained in these heterosupramolecular triads. Clearly, the incorporation of a solid substrate is very beneficial in this respect. The assemblies obtained therefore clearly behave as heterosupramolecular systems.

The last aspect to be considered is the incident-photon-to-current-efficiency data shown in Figure 8. The action spectra for the immobilized ruthenium complexes follow closely the absorption spectra as expected. For **TiO_2−RuOs** however, no photocurrent was obtained. This is not unexpected and can be explained by the oxidation potential of the osmium center which is too low to allow for effective scavenging of Os(III) by I^-. Kinetically, this is evident from Figure 9 which shows that in the presence of iodide, the re-formation of Ru(II)Ru(II) from Ru(II)Ru(III) is much faster than that of Ru(II)Os(II) from Ru(II)Os(III). One interesting observation is that the IPCE for **TiO_2−RuRu** is about half of that observed for the assembly incorporating the mononuclear species **TiO_2−Ru**. The reasons for this are not clear at present. The decreased efficiency may be caused by the increased size of the molecular component. The extinction coefficient of **RuRu** at its absorption maximum is roughy twice that of **Ru** (see Experimental Part). Because the optical densities of **TiO_2−RuRu** and **TiO_2−Ru** in the experiments carried out were approximately the same and because one may assume that the molecular size of **RuRu** is about twice that of **Ru**, it is clear that for the surface modified with the dinuclear compound only half as many adsorbed species are present. This is consistent with the decrease in ICPE observed. Experiments are underway to further investigate this observation.

Conclusions

The results reported in this paper show that upon immobilization of a molecular dyad onto a solid substrate a substantial difference is observed between the photophysical processes observed for the heterotriad and those observed for the dyad in solution. The data also strongly indicate that direct injection from moieties not directly bound to the oxide surface can be efficient. Importantly, for the **TiO_2−RuOs** triad studied, no osmium-based emission is observed and injection from both the ruthenium and the osmium centers is faster than the laser pulse. An interesting observation is also that upon irradiation of **TiO_2−RuOs**, only one final product, TiO_2−Ru(II)Os(III), is obtained. In view of the potential of these modified surfaces as molecular devices, this is an important feature. More detailed studies are underway to differentiate between the direct and the indirect injection processes.

Acknowledgment. The authors thank the TMR Programme of the European Community for financial support (Grant No. TMR CT96-0076), Dr. M. Ward of the University of Bristol for the mass spectra, and Professor F. Scandola for his interest in this study.

IC0102743